Inorg. Chem. **2007**, *46*, 5678–5685

Alumazene Adducts with Pyridines: Synthesis, Structure, and Stability Studies

Jiri Lӧbl,[†] Alexey Y. Timoshkin,[‡] Trinh Cong,[‡] Marek Necas,[†] Herbert W. Roesky,[§] and Jiri Pinkas*,[†]

Department of Chemistry, Masaryk University, Kotlarska 2, CZ-61137 Brno, Czech Republic, Inorganic Chemistry Group, Department of Chemistry, St. Petersburg State University, University pr. 26, Old Peterhof 198504, Russia, and Institut für Anorganische Chemie, Universität Göttingen, Tammannstrasse 4, D-37077 Göttingen, Germany

Received March 13, 2007

Lewis acid–base adducts of the alumazene [2,6-(*i*-Pr)$_2$C$_6$H$_3$NAlMe]$_3$ (**1**) with pyridine (py) and 4-dimethylaminopyridine (dmap) were synthesized and structurally characterized: **1**(py)$_2$ (**2**), **1**(py)$_3$ (**3**), **1**(dmap)$_2$ (**4**), and **1**(py)(dmap) (**5**). The bisadducts **2**, **4**, and **5** form the *trans* isomers. The trisadduct **3** exhibits an unexpected *cis–cis* isomer and can be prepared only in the presence of excess py. The planarity of the alumazene ring is lost upon coordination of the Lewis base molecules. A comparison of the Al–N(base) bond distances and pyramidality at Al suggests the higher basicity of dmap. NMR spectroscopy confirms stability to dissociation of the bisadducts in solution while the trisadduct **3** is labile and converts to **2**. The thermodynamics of the adduct formation has been investigated experimentally and theoretically. Thermodynamic characteristics of the **1**(py)$_n$ (n = 2, 3) dissociation reactions in the temperature range 25–200 °C have been derived from the vapor pressure–temperature dependence measurements by the static tensimetric method. In all experiments, excess py was employed. Quantum chemical computations at the B3LYP/6-31G* level of theory have been performed for the **1**(py)$_n$ and model complexes [HAlNH]$_3$(py)$_n$ (n = 1–3). Obtained results indicate that for the gas phase adducts upon increasing the number of py ligands the donor–acceptor Al–N(py) distance increases in accord with decreasing donor–acceptor bond dissociation energies.

Introduction

Compounds containing Al−N moieties in their molecules are intensively studied as single source precursors for the CVD[1] or polymer pyrolysis[2] fabrication of AlN materials. Two most frequently used families of compounds are alane−amine adducts, R_3Al-NR_3, and aminoalanes, $[R_2Al-NR_2]_n$. However, the molecular species most closely related to AlN are iminoalanes, $[RAl-NR]_n$,[3] that form a diverse group of cage compounds for $n \geq 4$.[4] Oligomers with smaller n are rare and require steric and/or electronic stabilization.[5] One example is trimeric iminoalane 1,3,5-trimethyl-2,4,6-tris(2,6-di*iso*propylphenyl)alumazene (**1**).[6] Alumazene **1** belongs to

* To whom correspondence should be addressed. E-mail: jpinkas@chemi.muni.cz. Phone: +420549496493. Fax: +420549492443.
[†] Masaryk University.
[‡] St. Petersburg State University.
[§] Universität Göttingen.

(1) (a) Barron A. R. In *CVD of Nonmetals*; Rees, W. S., Jr., Ed.; VCH: Weinheim, 1996; p 300. (b) Jones, A. C.; O'Brien, P. *CVD of Compound Semiconductors*; VCH: Weinheim, 1997; p 296.
(2) (a) Janik, J. F.; Paine, R. T. *J. Organomet. Chem.* **1993**, *449*, 39−44. (b) Mori, Y.; Kumakura, Y.; Sugahara, Y. *J. Organomet. Chem.* **2006**, *691*, 4289−4296. (c) Saito, Y.; Sugahara, Y.; Kuroda, K. *J. Am. Ceram. Soc.* **2000**, *83*, 2436−2440. (d) Sauls, F. C.; Interrante, L. V. *Coord. Chem. Rev.* **1993**, *128*, 193−207.
(3) Timoshkin, A. Y. *Coord. Chem. Rev.* **2005**, *249*, 2094−2131.
(4) Alwassil, A. A. I.; Hitchcock, P. B.; Sarisaban, S.; Smith, J. D.; Wilson, C. L. *J. Chem. Soc., Dalton Trans.* **1985**, 1929−1934.
(5) (a) Hardman, N. J.; Cui, C.; Roesky, H. W.; Fink, W. H.; Power, P. P. *Angew. Chem., Int. Ed.* **2001**, *40*, 2172−2174. (b) Wright, R. J.; Phillips, A. D.; Allen, T. L.; Fink, W. H.; Power, P. P. *J. Am. Chem. Soc.* **2003**, *125*, 1694−1695. (c) Wright, R. J.; Brynda, M.; Fettinger, J. C.; Betzer, A. R.; Power, P. P. *J. Am. Chem. Soc.* **2006**, *128*, 12498−2509. (d) Schulz, S.; Häming, L.; Herbst-Irmer, R.; Roesky, H. W.; Sheldrick, G. M. *Angew. Chem., Int. Ed.* **1994**, *33*, 969−970. (e) Schulz, S.; Thomas, F.; Priesmann, W. M.; Nieger, M. *Organometallics* **2006**, *25*, 1392−1398. (f) Schulz, S.; Voigt, A.; Roesky, H. W.; Häming, L.; Herbst-Irmer, R. *Organometallics* **1996**, *15*, 5252−5253. (g) Wehmschulte, R.; Power, P. P. *J. Am. Chem. Soc.* **1996**, *118*, 791−797. (h) Wehmschulte, R.; Power, P. P. *Inorg. Chem.* **1998**, *37*, 6906−6911. (i) Wehmschulte, R.; Power, P. P. *Inorg. Chem.* **1996**, *35*, 2717−2718. (j) Fisher, J. D.; Shapiro, P. J.; Yap, G. P. A.; Rheingold, A. L. *Inorg. Chem.* **1996**, *35*, 271−272. (k) Uhl, W.; Molter, J.; Koch, R. *Eur. J. Inorg. Chem.* **1999**, 2021−2027. (l) Bauer, T.; Schulz, S.; Hupfer, H.; Nieger, M. *Organometallics* **2002**, *21*, 2931−2939. (m) Bauer, T.; Schulz, S.; Nieger, M. *Z. Anorg. Allg. Chem.* **2004**, *630*, 1897−1810.

10.1021/ic700488p CCC: $37.00
Published on Web 06/13/2007

a class of compounds that attracted considerable attention. These are inorganic analogues of benzene: borazine,[7] boraphosphabenzene,[8] and alumazene.[6] They possess a central six-membered core $(RM-ER')_3$ which is isoelectronic with C_6H_6. The M−E bond distances in these rings are equalized. However, their degree of delocalization is much different from that of benzene and has been studied by computational and experimental methods. Alumazene **1** was shown to possess the lowest value of stabilization energy, and calculated ring currents were localized on N atoms.[9] Therefore, the reactivity in this series varies quite widely. In contrast to borazines, where delocalization of the N lone pairs to empty B orbitals is considerable, or boraphosphabenzenes, where both bonding partners possess similar electronegativity, **1** features highly polar Al−N bonds and N-localized electron pairs. As a result, borazines do not form any adducts with Lewis bases that would coordinate to the B centers while alumazene coordinates metallocene trifluorides,[10] $Me_3SiOP(O)O_2^{2-}$,[11] $OPPh_3$,[12] $OP(OMe)_3$,[13] and $MeS(O)_2O^-$.[14] Nitriles coordinate weakly to **1**, and bis- (*cis* and *trans*) and trisadducts were recently structurally authenticated.[15]

We were interested in probing the acidity of **1** as a trifunctional Lewis acid and in studying the influence of sequential coordination of Lewis bases on acidity of the remaining Lewis acid centers in the molecule. Furthermore, the possibility of inducing ring rearrangement of alumazene and the formation of smaller [RAl═NAr] oligomers stabilized by the base is worth considering.[16] We report here structural, spectroscopic, and computational results on the studies of reactions of **1** with strong N bases: pyridine (py) and 4-dimethylaminopyridine (dmap). We selected these pyridines as common Lewis bases that were frequently studied in interactions with group 13 acids, and literature data are available for a comparison.[17]

Dmap is one of the strongest Brønsted bases among pyridine derivatives.[18] Adducts of dmap with AlR_3 (R = Me, *t*-Bu, Cl)[19] and other group 13 acids were recently reported.

We established the molecular structures for bis- and trisadducts of **1** with py and dmap and studied the stability of these acid−base complexes in solution by NMR spectroscopy. Furthermore, we investigated the dissociation of the py adducts by the static tensimetric method. Also, the donor−acceptor bond dissociation energies were estimated by quantum chemical calculations.

Experimental Section

Reagents and General Procedures. All experiments were performed under strictly anaerobic and anhydrous conditions by combination of standard Schlenk techniques and an M. Braun Unilab glove box filled with nitrogen. The box atmosphere was maintained under 1 ppm of both O_2 and H_2O. Alumazene **1** was synthesized as previously reported.[6,20] Toluene was predried over NaOH and freshly distilled from sodium/benzophenone under nitrogen. Pyridine (Fluka) was predried over KOH and distilled from phosphorus pentoxide. 4-Dimethylaminopyridine (Merck) was used as received. Benzene-d_6 and THF-d_8 were distilled from Na/K alloy and degassed prior to use. Chloroform-d_1 was distilled from phosphorus pentoxide and degassed prior to use.

Instrumentation. Room temperature ^1H and $^{13}C\{^1H\}$ NMR spectra were obtained in C_6D_6, THF-d_8 or $CDCl_3$ solutions on Bruker Avance DRX 500, 300, and 200 MHz spectrometers. The ^1H and $^{13}C\{^1H\}$ NMR spectra were referenced to the residual proton signals or carbon resonances of benzene-d_6 (7.15 and 128.0, respectively), chloroform-d_1 (7.24 and 77.0, respectively) or tetrahydrofurane-d_8 (1.73 and 25.3, respectively). Diffraction data for **2** to **3** were collected on a Kuma KM-4 four-circle CCD diffractometer with graphite-monochromated Mo Kα radiation (λ = 0.71073 Å) and processed with the Xcalibur data reduction package.[21] The structures were solved by direct methods and refined using a SHELXTL program package.[22] The hydrogen atoms were placed in calculated idealized positions with isotropic temperature factors and refined as riding model. In case of **4**, the molecules of solvent (toluene) were affected by considerable disorder which was resolved using standard SHELX restraints. In figures, the thermal ellipsoids were drawn at the 50% probability level, and hydrogen atoms were omitted for clarity. The infrared spectra were recorded as KBr pellets on an EQUINOX 55/S/NIR FTIR spectrometer. EI (70 eV) mass spectra were obtained with Finnigan MAT Trio 1000 or Finnigan MAT 8230. Elemental analyses were carried out by the Analytisches Labor des Anorganischen Instituts, Göttingen. Melting points were obtained in sealed nitrogen-filled capillaries and are uncorrected.

(6) (a) Waggoner, K. M.; Hope, H.; Power, P. P. *Angew. Chem., Int. Ed. Engl.* **1988**, *27*, 1699−1700. (b) Waggoner, K. M.; Power, P. P. *J. Am. Chem. Soc.* **1991**, *113*, 3385−3393. (c) Power, P. P. *J. Organomet. Chem.* **1990**, *400*, 49−69.

(7) Niedenzu, K.; Dawson, J. W. *Boron-Nitrogen Compounds*; Springer-Verlag: Berlin, 1965; pp 85−102.

(8) (a) Dias, H. V. R.; Power, P. P. *Angew. Chem., Int. Ed. Engl.* **1987**, *26*, 1270−1271. (b) Dias, H. V. R.; Power, P. P. *J. Am. Chem. Soc.* **1989**, *111*, 144−148.

(9) (a) von Rague Schleyer, P.; Jiao, H.; van Eikema Hommes, N. J. R.; Malkin, V. G.; Malkina, O. L. *J. Am. Chem. Soc.* **1997**, *119*, 12669−12670. (b) Engelberts, J. J.; Havenith, R. W. A.; van Lenthe, J. H.; Jenneskens, L. W.; Fowler, P. W. *Inorg. Chem.* **2005**, *44*, 5266−5272. (c) Matsunaga, N.; Cundari, T. R.; Schmidt, M. W.; Gordon. M. S. *Theor. Chim. Acta* **1992**, *83*, 57−68.

(10) (a) Wessel, H.; Rennekamp, C.; Roesky, H. W.; Montero, M. L.; Müller, P.; Usón, I. *Organometallics* **1998**, *17*, 1919−1921. (b) Wessel, H.; Montero, M. L.; Rennekamp, C.; Roesky, H. W.; Yu, P.; Usón, I. *Angew. Chem., Int. Ed.* **1998**, *37*, 843−845.

(11) Pinkas, J.; Löbl, J.; Dastych, D.; Necas, M.; Roesky, H. W. *Inorg. Chem.* **2002**, *41*, 6914−6918.

(12) Löbl, J.; Necas, M.; Pinkas, J. *Main Group Chem.* **2006**, *5*, 79−88.

(13) Pinkas, J.; Wessel, H.; Yang, Y.; Montero, M. L.; Noltemeyer, M.; Fröba, M.; Roesky, H. W. *Inorg. Chem.* **1998**, *37*, 2450−2457.

(14) Löbl, J.; Pinkas, J.; Roesky, H. W.; Plass, W.; Görls, H. *Inorg. Chem.* **2006**, *45*, 6571−6573.

(15) Löbl, J.; Necas, M.; Plass, W.; Roesky, H. W.; Pinkas, J. Unpublished data.

(16) Rivard, E.; Merrill, W. A.; Fettinger, J. C.; Power, P. P. *Chem. Commun.* **2006**, 3800−3802.

(17) (a) Healy, M. D.; Weirda, D. A.; Barron, A. R. *Organometallics* **1988**, *7*, 2543−2548. (b) Healy, M. D.; Ziller, J. W.; Barron, A. R. *J. Am. Chem. Soc.* **1990**, *112*, 2949−2954. (d) Lichtenberger, D. L.; Hogan, R. H.; Healy, M. D.; Barron, A. R. *Organometallics* **1991**, *10*, 609−614. (e) Thomas, F.; Schulz, S.; Nieger, M. *Eur. J. Inorg. Chem.* **2001**, 161−166.

(18) (a) Nabavizadeh, S. M.; Akbari, A.; Rashidi, M. *Eur. J. Inorg. Chem.* **2005**, 2368−2375. (b) Nabavizadeh, S. M. *Inorg. Chem.* **2003**, *42*, 4204−4208.

(19) Thomas, F.; Bauer, T.; Schulz, S.; Nieger, M. *Z. Anorg. Allg. Chem.* **2003**, *629*, 2018−2027.

(20) Pinkas, J. In *Inorganic Experiments*, 2nd ed.; Woollins, J. D., Ed.; Wiley-VCH: Weinheim, 2003; pp 357−359.

(21) *Xcalibur CCD System, CrysAlis Software System*, version 1.170; Oxford Diffraction Ltd: Oxford, U.K., 2003.

(22) *SHELXTL*, version 5.10; Bruker AXS Inc.: Madison, WI, 1997.

Vapor Pressure Measurements. Tensimetry studies were performed by a static method with a glass membrane as null manometer.[23] A sealed chamber containing investigated substances was heated in a furnace at a rate of about 0.5 °C min^{-1}. The temperature was controlled by means of two chromel−alumel thermocouples, and the vapor pressure was measured with a mercury manometer. Because of the high air and moisture sensitivity of **1**, introduction of the samples for all experiments has been performed in a glass apparatus under vacuum (~10^{-5} Torr).

Computational Details. All structures have been fully optimized at the B3LYP/6-31G* level of theory[24,25] and verified to be minima on the potential energy surface. The Gaussian 03 program package[26] has been employed throughout. Standard enthalpies were obtained by taking into account zero point energies and thermal corrections. Zero point energies, thermal corrections, and standard entropies have been computed by standard statistical thermodynamic methods using the ideal gas rigid rotor-harmonic oscillator approximations using optimized geometries and computed vibrational frequencies (unscaled).

Synthesis of [2,6-(*i*-Pr)$_2$C$_6$H$_3$NAlMe]$_3$(C$_5$H$_5$N)$_2$ (2). Alumazene **1** (0.305 g, 0.468 mmol) was dissolved in dry and deoxygenated toluene (10 mL). After addition of neat pyridine (0.109 g, 1.38 mmol), the solution turned yellow. Colorless X-ray quality crystals (0.124 g, 0.153 mmol, 32.8%) formed after 24 h at 22 °C. Mp: 250.0−251.9 °C. ^{1}H NMR (500 MHz, chloroform-d_1, 223 K): δ −1.06 (s, ^{13}C satellites, $^1J_{CH}$ = 115.4 Hz, AlCH_3, 3H), −0.78 (s, ^{13}C satellites, $^1J_{CH}$ = 111.4 Hz, pyAlCH_3, 6H), 0.25 (d, $^3J_{HH}$ = 6.3 Hz, (CH_3)$_2$CH, 6H), 0.69 (d, $^3J_{HH}$ = 6.0 Hz, (CH_3)$_2$CH, 6H), 1.12 (d, $^3J_{HH}$ = 6.5 Hz, (CH_3)$_2$CH, 6H), 1.22 (d, $^3J_{HH}$ = 6.1 Hz, (CH_3)$_2$-CH, 6H), 1.34 (d, $^3J_{HH}$ = 6.4 Hz, (CH_3)$_2$CH, 6H), 1.53 (d, $^3J_{HH}$ = 6.1 Hz, (CH_3)$_2$CH, 6H), 3.50 (sept, $^3J_{HH}$ = 6.5 Hz, (CH$_3$)$_2$CH, 2H), 4.05 (sept, $^3J_{HH}$ = 6.5 Hz, (CH$_3$)$_2$CH, 2H), 4.33 (sept, $^3J_{HH}$ = 6.5 Hz, (CH$_3$)$_2$CH, 2H), 7.00 (mult, 5H), 7.10 (d, $^3J_{HH}$ = 7.3 Hz, 2H), 7.25 (d, $^3J_{HH}$ = 6.3 Hz, 2H), 7.35 (mult, 2H), 7.43 (t, $^3J_{HH}$ = 7.5 Hz, 1H), 7.50 (t, $^3J_{HH}$ = 6.5 Hz, 4H), 8.01 (t, $^3J_{HH}$ = 7.55 Hz, 2H), 8.27 (br s, *H*C-2 py, 2H). ^{13}C{^{1}H} NMR (125.78 MHz, chloroform-d_1, 223 K, onax = on-C_2 axis, outax = out-of-C_2 axis): δ −12.04 (br s, Al*C*H$_3$), −7.81 (br s, pyAl*C*H$_3$), 22.98 (s), 23.51 (s), 24.69 (s), 24.92 (s), 25.15 (s), 25.28 (s) (6×(*C*H$_3$)$_2$CH), 27.18 (s), 27.26 (s), 27.80 (s) (3×(CH$_3$)$_2$*C*H), 118.92 (s, C-4 onax-dipp), 119.74 (s, C-4 outax-dipp), 122.55 (s), 122.71 (s), 122.88 (s) (3×C-3 dipp), 124.79 (s, C-3 py), 140.23 (s, C-4 py), 143.63 (s), 144.09 (s), 144.87 (s) (3×C-2 dipp), 148.09 (s, C-1 outax-dipp), 148.26 (s, C-1 onax-dipp), 151.72 (s, C-2 py). MS [EI, *m*/*z* (rel. int)] 652 (100, **1**$^+$). Mp: 250.0−251.9 °C. Anal. Calcd for C$_{49}$H$_{70}$Al$_3$N$_5$: C, 72.65; H, 8.71; Al, 9.99; N, 8.65. Found: C, 74.15; H, 8.63; Al, 9.38; N, 7.56.

Synthesis of [2,6-(*i*-Pr)$_2$C$_6$H$_3$NAlMe]$_3$(C$_6$H$_5$N)$_3$ (3). Alumazene **1** (0.169 g, 0.259 mmol) was dissolved in dry and deoxygenated toluene (5 mL), and then pyridine was added dropwise (1.418 g, 17.93 mmol, 1:69). A yellow solution was formed immediately. After 3 days, the solution was concentrated by evaporation of approximately 1 mL of solvent. Colorless X-ray quality crystals (0.152 g, 0.171 mmol, 66%) were formed after 10 days at 22 °C. The crystals for the X-ray analysis were selected and picked from the mother liquor. Adduct **3** is unstable in the absence of excess of pyridine. The X-ray diffraction experiment on crystals grown on the flask walls outside the solution revealed the bisadduct **2**. Similarly, the ^{1}H NMR spectrum of crystals removed from the mother liquor and dried in vacuum corresponds to **2**, and their melting points are identical (mp: 250.1−251.5 °C).

Synthesis of [2,6-(*i*-Pr)$_2$C$_6$H$_3$NAlMe]$_3$(dmap)$_2$ (4). Alumazene **1** (0.302 g, 0.464 mmol) was dissolved in dry and deoxygenated toluene (10 mL). Solid 4-dimethylaminopyridine (0.124 g, 1.015 mmol) was added to this solution. Colorless X-ray quality crystals (0.262 g, 0.292 mmol, 63.1%) formed after 12 h at 22 °C. ^{1}H NMR (300 MHz, chloroform-d_1): δ −1.19 (s, ^{13}C satellites, $^1J_{CH}$ = 116.4 Hz, AlCH_3, 3H), −0.89 (s, ^{13}C satellites, $^1J_{CH}$ = 111.2 Hz, (dmap)-AlCH_3, 6H), 0.45 (br s (CH_3)$_2$CH, 6H), 0.81 (d, $^3J_{HH}$ = 6.6 Hz, (CH_3)$_2$CH, 6H), 1.10 (br s, (CH_3)$_2$CH, 6H), 1.19 (d, $^3J_{HH}$ = 6.7 Hz, (CH_3)$_2$CH, 6H), 1.24 (br s, (CH_3)$_2$CH, 6H), 1.41 (br s, (CH_3)$_2$-CH, 6H), 3.03 (s, ^{13}C satellites, $^1J_{CH}$ = 137.5 Hz, (CH_3)$_2$N, 12H), 3.61 (br s, (CH$_3$)$_2$CH, 2H), 4.19 (sept, $^3J_{HH}$ = 6.7 Hz, (CH$_3$)$_2$CH, 2H), 4.25 (br s, (CH$_3$)$_2$CH, 2H), 6.31 (d, $^3J_{HH}$ = 6.9 Hz, H-3 dmap, 4H), 6.84−7.33 (br m, C$_6$*H*$_3$), 7.69 (d, $^3J_{HH}$ = 6.6 Hz, H-2 dmap, 4H). ^{13}C{^{1}H} NMR (75.48 MHz, chloroform-d_1, onax = on-C_2 axis, outax = out-of-C_2 axis): δ −11.76 (br s, Al*C*H$_3$), −7.18 (br s, (dmap)Al*C*H$_3$), 23.52 (br s), 24.22 (br s), 25.24 (s), 25.50 (s) ((*C*H$_3$)$_2$CH), 27.35 (s), 27.54 (br s) ((CH$_3$)$_2$*C*H), 39.15 (s, (*C*H$_3$)$_2$N), 105.77 (s, C-3, dmap), 118.45 (s, C-4 onax dipp), 119.52 (s, C-4 outax dipp), 122.64 and 122.78 (2:1 s, C-3 dipp), 144.31 (br s), 144.54 (br s), and 145.44 (s) (3×C-2 dipp), 147.88 (s, C-2 dmap), 149.61 and 153.77 (2:1 s, C-1 dipp), 155.08 (s, C-4 dmap). Mp. 264.6−266.0 °C.

Synthesis of [2,6-(*i*-Pr)$_2$C$_6$H$_3$NAlMe]$_3$(C$_5$H$_5$N)(dmap) (5). Alumazene **1** (0.306 g, 0.470 mmol) was dissolved in dry and deoxygenated toluene (10 mL). Addition of solid dmap (0.055 g, 0.45 mmol) and its dissolution were followed by a dropwise addition of pyridine (0.034 g, 0.43 mmol). The solution color turned yellow. After reducing solvent volume under vacuum to 6 mL, colorless X-ray quality crystals (0.214 g, 0.251 mmol, 58.3%) formed after 48 h at 22 °C. ^{1}H NMR (500 MHz, chloroform-d_1, 223 K): δ −1.21, −1.19, −1.16 (3×s, AlCH_3); −0.96, −0.94, −0.88, −0.86 (4×s, base-AlCH_3); 0.09 (6.6 Hz), 0.16 (6.7), 0.38 (6.4), 0.45 (6.7), 0.48 (6.5), 0.60 (6.5), 0.75 (4.8), 0.89 (6.2), 0.96 (6.4), 1.01 (6.2), 1.02 (4.3), 1.05 (6.5), 1.06 (6.5), 1.12 (6.8), 1.15 (5.4), 1.20 (5.8), 1.21 (5.6), 1.25 (6.7), 1.31 (6.4), 1.37 (6.2), 1.38 (6.1), 1.44 (6.3), (22×d, $^3J_{HH}$ Hz, (CH_3)$_2$CH); 3.01 and 3.06 (2×s, ^{13}C satellites, $^1J_{CH}$ = 140 Hz, N(CH_3)$_2$); 3.40 (sept, $^3J_{HH}$ = 6.6 Hz, (CH$_3$)$_2$CH); 3.60 (mult, (CH$_3$)$_2$CH); 3.74 (br sept, $^3J_{HH}$ = 5.4 Hz, (CH$_3$)$_2$CH); 3.95 (br sept, $^3J_{HH}$ = 6.3 Hz, (CH$_3$)$_2$CH); 4.16, 4.23, 4.33 (3×mult, (CH$_3$)$_2$CH); 6.18 (d, $^3J_{HH}$ = 6.5 Hz); 6.31 (d, $^3J_{HH}$ = 5.4 Hz); 6.88−6.92 (mult); 6.94 (mult); 7.00 (d, $^3J_{HH}$ = 7.4 Hz); 7.06 (d, $^3J_{HH}$ = 7.3 Hz); 7.11 (mult); 7.16 (mult); 7.25 (d, $^3J_{HH}$ = 7.7 Hz); 7.34 (t, $^3J_{HH}$ = 7.5 Hz); 7.41 (t, $^3J_{HH}$ = 6.6 Hz); 7.52 (t, $^3J_{HH}$ = 6.5 Hz); 7.93 (t, $^3J_{HH}$ = 7.6 Hz); 8.00 (t, $^3J_{HH}$ = 7.6 Hz); 8.18 (br s); 8.59 (br s). ^{13}C{^{1}H} NMR (125.77 MHz, chloroform-d_1, 223 K): δ

(23) Suvorov, A. V. *Thermodynamic Chemistry of Vapor State (Thermodynamicheskaia khimia paroobraznogo sostoiania)*; Khimia: Leningrad, 1970.
(24) Becke, A. D. *J. Chem. Phys.* **1993**, *98*, 5648−5652.
(25) Lee, C.; Yang, W.; Parr, R. G. *Phys. Rev. B* **1988**, *37*, 785−789.
(26) Frisch, M. J.; Trucks, G. W.; Schlegel, H. B.; Scuseria, G. E.; Robb, M. A.; Cheeseman, J. R.; Montgomery, J. A., Jr.; Vreven, T.; Kudin, K. N.; Burant, J. C.; Millam, J. M.; Iyengar, S. S.; Tomasi, J.; Barone, V.; Mennucci, B.; Cossi, M.; Scalmani, G.; Rega, N.; Petersson, G. A.; Nakatsuji, H.; Hada, M.; Ehara, M.; Toyota, K.; Fukuda, R.; Hasegawa, J.; Ishida, M.; Nakajima, T.; Honda, Y.; Kitao, O.; Nakai, H.; Klene, M.; Li, X.; Knox, J. E.; Hratchian, H. P.; Cross, J. B.; Bakken, V.; Adamo, C.; Jaramillo, J.; Gomperts, R.; Stratmann, R. E.; Yazyev, O.; Austin, A. J.; Cammi, R.; Pomelli, C.; Ochterski, J. W.; Ayala, P. Y.; Morokuma, K.; Voth, G. A.; Salvador, P.; Dannenberg, J. J.; Zakrzewski, V. G.; Dapprich, S.; Daniels, A. D.; Strain, M. C.; Farkas, O.; Malick, D. K.; Rabuck, A. D.; Raghavachari, K.; Foresman, J. B.; Ortiz, J. V.; Cui, Q.; Baboul, A. G.; Clifford, S.; Cioslowski, J.; Stefanov, B. B.; Liu, G.; Liashenko, A.; Piskorz, P.; Komaromi, I.; Martin, R. L.; Fox, D. J.; Keith, T.; Al-Laham, M. A.; Peng, C. Y.; Nanayakkara, A.; Challacombe, M.; Gill, P. M. W.; Johnson, B.; Chen, W.; Wong, M. W.; Gonzalez, C.; Pople, J. A. *Gaussian 03*, revision B.01; Gaussian, Inc.: Wallingford, CT, 2004.

Table 1. Crystallographic Data and Refinement Parameters for Compounds **2**−**5**

	2	**3**	**4**	**5**
empirical formula	$C_{56}H_{78}Al_3N_5$	$C_{68}H_{91}Al_3N_6$	$C_{81}H_{104}Al_3N_7$	$C_{58}H_{83}Al_3N_6$
fw	902.17	1073.41	1256.65	945.24
cryst syst	triclinic	orthorhombic	orthorhombic	triclinic
space group	$P\bar{1}$	$P2_12_12_1$	*Pbcn*	$P\bar{1}$
a [Å]	12.847(3)	12.619(1)	46.001(9)	12.768(3)
b [Å]	13.472(3)	20.363(1)	16.707(3)	13.144(3)
c [Å]	16.384(3)	24.109(1)	19.466(4)	18.283(4)
α [deg]	91.90(3)	90	90	97.29(3)
β [deg]	103.11(3)	90	90	109.16(3)
γ [deg]	96.52(3)	90	90	91.13(3)
V [Å^3]	2738.8(10)	6195.0(2)	14960(5)	2868.7(11)
Z	2	4	8	2
ρ [Mg/m^3]	1.094	1.151	1.116	1.094
μ [mm^{-1}]	0.108	0.106	0.097	0.106
reflns collected/unique	17974/9360	59798/10901	80498/13154	20067/10004
data/params	9360/578	10901/695	13154/830	10004/606
final *R* indices [$I > 2\sigma(I)$]	0.0628/0.1624	0.0471/0.1138	0.0830/0.1917	0.0607/0.0953
R indices (all data)	0.0956/0.1809	0.0819/0.1243	0.1644/0.2312	0.2292/0.1340
$\Delta\rho_{max}/\Delta\rho_{min}$ [e Å^{-3}]	1.052/−0.476	0.512/−0.361	0.644/−0.457	0.217/−0.239

−12.04, −11.98, −11.91 (3×s, Al*C*H$_3$); −9.7, −7.82, −5.73 (br s, base-Al*C*H$_3$). For the listing of remaining resonances, see Supporting Information. Mp: 273.1−274.4 °C.

Results and Discussion

The bisadducts **2**, **4**, and **5** were prepared by direct reactions of Lewis acidic **1** with a particular pyridine base. The products crystallized out of the reaction solution at ambient temperature in moderate to good yields. X-ray quality crystals were selected from the crop of product. Their molecular structures were established by single-crystal X-ray diffraction experiments. Crystal data and refinement parameters for structures **2**, **3**, **4**, and **5** are given in Table 1.

For the formation of the trisadduct **3**, a 1:3 molar ratio of **1** to py was insufficient, and the isolation required excess pyridine (1:69). Crystals formed in the mother liquor were identified by the single-crystal X-ray diffraction experiments as **3** while crystals sticking to the walls of the Schlenk flask without the contact with the solution or solid dried under vacuum were proven to be the bisadduct **2** by X-ray diffraction measurements, ^{1}H NMR spectroscopy, and the melting point. This suggests a low stability of the third coordinative Al−N bond as discussed below. The solid bisadducts **2**, **4**, and **5** have relatively high melting points (250−274 °C).

The bisadducts **2**, **4**, and **5** crystallized out in the form of *trans* isomers as the two bases coordinated by their electron lone pair at N to the opposite faces of the alumazene ring. Their molecular structures are shown in Figures 1−3, and selected metric parameters are gathered in Table 2. The same configuration was observed in the bisadduct **1**(OPPh$_3$)$_2$.[12] In contrast, the *cis* isomers were observed in the bisadducts of **1** with 2,6-dihalogenobenzonitriles,[15] where *π*−X intramolecular interactions can be responsible for the stabilization of the *cis* geometry. An unprecedented *cis* isomer was found for **1**[OP(OMe)$_3$]$_2$.[13] The shapes of the cyclic Al$_3$N$_3$ cores in **2**, **4**, and **5** are similar with one N atom displaced from the ring plane while **3** forms a boat conformer. In the bisadducts, the rms deviations from the Al1−N1−Al2−N3−Al3 planes are 0.030 Å (**2**), 0.060 Å (**4**), and 0.037 Å (**5**). The nitrogens N2 connecting the two four-coordinated Al2 and Al3 atoms deviate from those planes by 0.587 Å (**2**), 0.578 Å (**4**), and 0.627 Å (**5**). Note that the noncoordinated skeleton of alumazene **1** is ideally planar.

The sums of the valence angles on the noncoordinated Al atoms in **2**, **4**, and **5** are very close to 360° (within 0.3°), indicating the sp^2 hybridization and a planar arrangement. Upon coordination, the bonding environments at Al2 and Al3 approach tetrahedral, as can be seen from a comparison of the intracyclic N−Al−N angles including either noncoordinated Al1, or coordinated Al2 or Al3 atoms (Table 2). The passage from trigonal to tetrahedral environments is accompanied by lengthening in the internal Al−N bonds. In **3**, the Al centers are all four-coordinate, and the distribution of bond lengths and angles is thus more uniform. Concurrently, all internal Al−N bonds are considerably shorter than the coordinative Al−N bonds, in agreement with

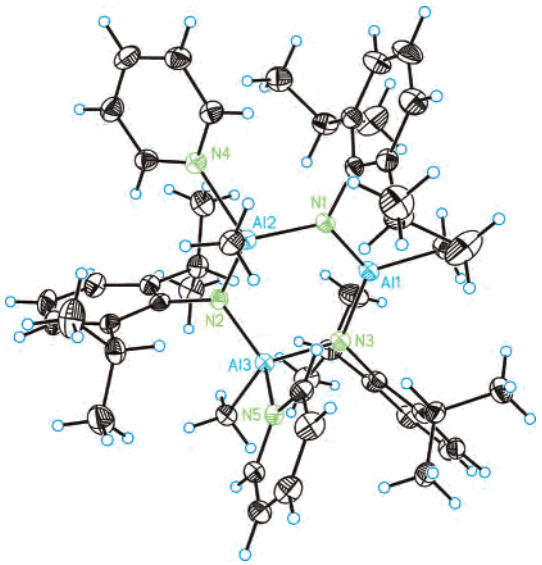

Figure 1. Molecular structure of **2** with all atoms included. The py ligands adopt a *trans* geometry.

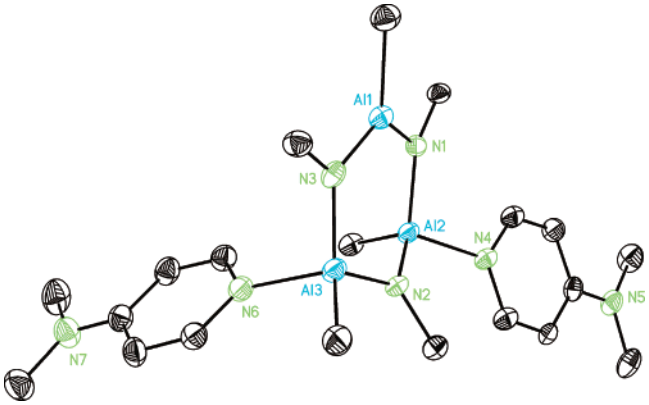

Figure 2. Molecular structure of **4**. All atoms of the dipp groups, except the *ipso*-C, were omitted for clarity. The N2 atom bridging the coordinated Al2 and Al3 centers is displaced from the alumazene plane.

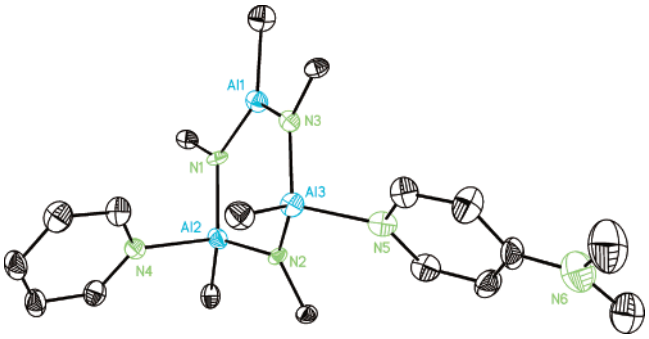

Figure 3. Molecular structure of **5**. All atoms of the dipp groups, except the *ipso*-C, were omitted for clarity. The coordination geometry at Al2 is much less distorted from the trigonal planar by coordinated py than the tetrahedral environment around Al3 with a bound dmap molecule.

Table 2. Selected Average Bond Lengths (Å) and Angles (deg) for Prepared Compounds (**2**−**5**) and the Parent Noncoordinated Alumazene (**1**) Skeleton[a]

length/angle	**1**[b]	**2**[c]	**3**	**4**[c]	**5**[c]
Al1−N(int)	1.782(4)	1.813	1.845	1.780	1.811
Al2−N(int)	1.782(4)	1.860	1.857	1.843	1.855
Al3−N(int)	1.782(4)	1.863	1.854	1.835	1.853
Al−N(ext)		2.064(3), 2.040(3)	2.044, 2.103(2)	2.004	2.037
N1−Al1−N3	115.3(5)	118.8(1)	109.3(1)	122.0(2)	118.5(2)
N1−Al2−N2	115.3(5)	108.1(1)	112.8(1)	108.1(2)	111.5(2)
N2−Al3−N3	115.3(5)	111.8(1)	112.7(1)	108.6(2)	107.4(2)

[a] The intracyclic nitrogen atoms are labeled int, and the extracyclic (donor) nitrogen atoms are labeled ext. [b] The values are taken from ref 6. [c] The Al2, Al3 are coordinated by N-donating bases. Al1 is the noncoordinated atom; for atom numbering scheme see Figures 1−4.

the seminal study of Haaland.[27] However, there are differences within the coordinative bonds, following the difference in the basicity of particular N-bases.

The two Al−N coordination bond distances in **2** are slightly different (2.064(3) and 2.040(3) Å) while in **4** they are equal within 3σ (av 2.004(6) Å) and considerably shortened as the strong dmap base binds more tightly than py. Similar distances were observed in X_3Al−dmap adducts: 2.015(3), 1.901(9), and 2.017(2) Å)[19] for X = Me, Cl, and *t*-Bu, respectively. The corresponding Al−C bond distances in **2** (av 1.997(4) Å) are slightly elongated in comparison with those in **1** (1.978(15) Å)[6] while those in in **4** (av 1.969(7) Å) are unchanged. The coordination environments around the two four-coordinate Al centers slightly differ in **2** (sum of angles 342.9° and 344.7° at Al2 and Al3, respectively) and are less distorted from sp^2 than in **4** where both Al atoms have the same degree of pyramidality (av sum of angles 341.2°). The metric features in the molecular structure of the mixed bisadduct **5** of py and dmap (Figure 3) agree with the higher basicity of dmap. Although the Al−N bond lengths to py and dmap are indistinguishable on the 3σ grounds (av 2.037(6) Å) the pyramidality of dmap coordinated atom Al3 (340.2°) is higher than Al2 (345.5°) bound to py.

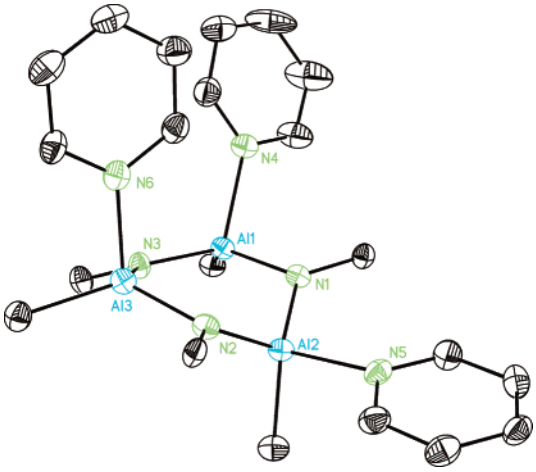

Figure 4. Molecular structure of **3**. All atoms of the dipp groups, except the *ipso*-C, were omitted for clarity. All-*cis* geometry is adopted by the three py donors.

Excess py in reaction with **1** induces the formation of crystalline trisadduct **3** whose molecular structure is depicted in Figure 4. The trisadduct features a *cis*−*cis* arrangement of the three py donors. The ring is folded to form a boat conformation with two py occupying axial positions and one pointing in equatorial direction. One of the py molecules is bound less tightly (Al1−N4, 2.103(2) Å) than the other two (av Al−N, 2.044(4) Å). These structural features can be attributed to the two py bases coordinating to the ring of **1** more strongly and diminishing the Lewis acidity of the remaining Al center.

The aromatic ring of one of the two (**2**, **4**, and **5**) or three (**3**) attached ligands is oriented in-plane (approximately aligned) with Al−C(methyl) bond. The relevant pairs of torsion angles C(ar)−N−Al−C(methyl) are −0.7(3)°/−179.5(2)° for **2**, 6.2(3)°/−170.1(2)° for **3**, 1.1(4)°/−175.0(4)° for **4**, and 5.0(5)°/−178.0(4)° for **5**. We suppose that the described consistency in the orientations of the ligand planes is related to the energy minima in the systems considerably crowded with aromatic rings. The aromatic rings of the other ligands are more or less out of the N−Al−C(methyl) planes, with dihedral angles 58.4°, 87.4°, and 48.4° for **2**, **4**, and **5**, respectively, and 59.5° and 78.2° for **3**. There are several intramolecular contacts between hydro-

(27) (a) Haaland, A. *Angew. Chem., Int. Ed. Engl.* **1989**, *28*, 992−1007. (b) Haaland, A. In *Chemistry of Aluminum*; Robinson, G. H., Ed.; VCH: Weinheim 1993; p 1.

gen atoms and aromatic rings. Among them, the interactions between C−H hydrogens of the ligands and the *ipso* carbons of the diisopropylphenyl groups are especially remarkable. The C−H···π interactions may be characterized by the C−H···C(*ipso*) distances, which are sometimes as short as 2.509 Å (**4**). Intermolecular C−H···π interactions are also responsible for the formation of larger aggregates in the solid state. Thus, we observed dimeric arrangement for **2**, while **3**, **4**, and **5** form polymeric chains, often including the molecules of solvent.

The stability to dissociation of the bisadducts **2**, **4**, and **5** in solution was studied by ^{1}H and ^{13}C{^{1}H} NMR spectroscopy. ^{1}H NMR spectrum of **2** measured at room temperature was complicated and not easily assignable. However, at −50 °C it shows only one set of resonances that exclude the presence of a *cis*/*trans* equilibrium. The bisadduct **4** displays sharp signals already at room temperature in concert with stronger bonding ability of dmap. The number of resonances in the spectra of **2** and **4** reflects the idealized symmetry point group C_2. There are 2 singlet resonances in a 1:2 integral ratio for the Al−Me; the weaker and more shielded one was assigned to the uncoordinated moiety. The comparison of the magnitude of direct C−H coupling constants in free alumazene **1** ($^1J_{CH}$ 118 Hz) and uncoordinated Al−Me in **2** and **4** (115.4 and 116.4 Hz, respectively) with the ones for the base-coordinated Al−Me moieties in **2** and **4** (111.4 and 111.2 Hz, respectively) shows a decrease in their values caused by diminished s-character in the C−H bonds that arises by lower electron withdrawing power of the alumazene ring coordinated by Lewis bases. A similar decrease from 117 to 110 Hz was observed in the $^1J_{CH}$ scalar coupling of the uncoordinated and coordinated Al−Me in the monoadduct **1**(OPPh$_3$).[12] Geminal Me groups in the 2,6-diisopropylphenyl (dipp) ligands serve as excellent reporters of molecular symmetry in solution. Their diastereotopic nature in the *trans* bisadduct molecules combined with the idealized C_2 axis passing through one of the three dipp rings resulted in the presence of 6 Me doublet resonances and 3 methine septets. This led us to exclude the possibility of the observed species being the *cis* isomer with C_s symmetry which would imply 4 inequivalent methine protons. From these data, we can conclude that the pyridines are attached to the Al centers and do not dissociate on the NMR time scale. The number and intensities of resonances in the ^{13}C{^{1}H} NMR spectra of **2** and **4** also reflect the C_2 molecular symmetry. One of the two Al−Me resonances is broadened and more deshielded (−7.81 (**2**), −7.18 (**4**) ppm) from the value for free **1** (−16.13 ppm) and was tentatively assigned to the four coordinated Al centers. The resonance of uncoordinated Al−Me is only slightly downfield shifted (−12.04 (**2**), −11.76 (**4**) ppm) from **1**. Six methyl and three methine resonances correspond well to the expected number of diastereotopic *i*-Pr group signals. Both C-1 and C-4 carbons of the dipp groups display two resonances in an approximate ratio 2:1, which is consistent with one of the dipp lying on the C_2 axis and the other two being in- and out-of-axis positions. Three resonances of the same intensity for both C-3 and C-2 atoms in the dipp rings attest again to the on/out-axis positions and concur with an expected slow rotation on the NMR time scale of the dipp groups around the C-1-N axes. Coordination to Al causes the py resonances of **2** to shift downfield; the largest change was observed for the C-4 signal (+5 ppm).

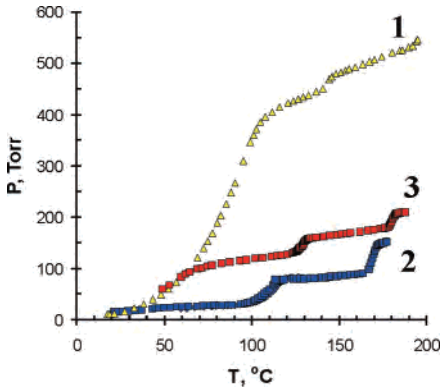

Figure 5. Vapor pressure−temperature dependence in alumazene−pyridine system. Only heating data points are given. Yellow points indicate first series (py/**1** ratio 20.8), blue points indicate second series (py/**1** ratio 3.3), and red points indicate third series (py/**1** ratio 5.5).

The mixed py/dmap bisadduct **5** displays at −50 °C seven resonances in the Al−Me region of the ^{1}H NMR spectrum. This may be interpreted as a result of the simultaneous presence of three bisadducts **2**, **4**, and **5** in the solution that arose by the base dissociation and exchange. A group of three signals at high field represents uncoordinated Al−Me moieties while four signals are shifted to lower field from −1 ppm by the base coordination. Considering diastereotopicity of the *i*-Pr groups, we expect 24 and 12 resonances in the CH$_3$ and CH regions, respectively, for the mixture of **2**, **4**, and **5**. Resolving 22 doublets of Me in the ^{1}H NMR and 12 methine signals in the ^{13}C{^{1}H} NMR spectra lends some support to this idea. In addition, two sets of the dmap resonances appeared in the ^{1}H and ^{13}C{^{1}H} NMR spectra.

Tensimetry Studies. Three series of measurements were performed with different alumazene-to-pyridine ratios; in all cases, excess py was employed (Figure 5). In a typical run, the vapor pressure of pure py was measured first in saturated and unsaturated vapor pressure region. Then, the ampule with **1** was mechanically broken. Yellow coloring was observed immediately, and the system was allowed to equilibrate overnight. Then, measurement of the vapor pressure−temperature dependence was performed by repeating heating/cooling cycles several times. At the first heating, thermal expansion of py occurred at much lower pressures, indicating that py has complexed with alumazene. Taking the differences in thermal expansion lines of the py before and after complexation, the formation of **3** was confirmed in each of the three series. At about 100 °C, the exponential increase of pressure occurred, followed by another thermal expansion line. We attribute this exponential increase to the release of the first mole of gaseous py from **3**, and formation of the solid **2**. The second exponential increase of pressure was observed at about 170 °C, followed by another thermal expansion line. We attribute this to the release of gaseous py from **2**. On cooling, the exponential decrease of the pressure was absent, and pressure followed along the thermal

Table 3. Experimentally Obtained Structural and Thermodynamic Properties for the Solid Compounds

compd	melting point, °C	R_{M-N}(ring), Å	R_{M-N}(py), Å	T, K	$\Delta H^{\circ}_{T}{}^{diss}$, kJ mol^{-1}	$\Delta S^{\circ}_{T}{}^{diss}$, J mol^{-1} K^{-1}
1 (s)	272	1.782(4)				
1(py)$_2$ (s)	251	1.845[a]	2.052[a]	451	91 ± 3	191 ± 7
1(py)$_3$ (s)	251	1.853[a]	2.07[a]	394	78 ± 3	180 ± 8

[a] Mean value.

Table 4. Predicted Structural and Thermodynamic Properties for the Gas-Phase Compounds at B3LYP/6-31G* Level of Theory

compd	R_{M-N}(ring), Å	R_{M-N}(py), Å	$\Delta H^{\circ}_{298}{}^{diss}$, kJ mol^{-1}	$\Delta S^{\circ}_{298}{}^{diss}$, J mol^{-1} K^{-1}	$T_{K=1}$, K
[HAlNH]$_3$	1.802				
[HAlNH]$_3$(py)	1.811[a]	2.095	81	153	527
trans-[HAlNH]$_3$(py)$_2$	1.819[a]	2.110[a]	69	154	450
trans-[HAlNH]$_3$(py)$_3$	1.827[a]	2.123[a]	57	161	356
1	1.819				
1(py)	1.834[a]	2.111	49	263	176
trans-**1**(py)$_2$	1.851[a]	2.128[a]	30	210	141
trans-**1**(py)$_3$	1.873[a]	2.167[a]	−22	252	

[a] Mean value.

expansion line. This indicates that gaseous py does not react with **2**. We attribute the difference between the heating and cooling runs to the fact that establishing of the equilibrium between gaseous py and solid **2** is kinetically limited due to slow diffusion of the pyridine vapors into the solid sample. However, repeating the heating/cooling cycles after an overnight equilibration showed good reproducibility between runs. This observation indicates that liquid py reacts with **2** overnight, which dovetails with the fact that trisadduct **3** is formed only when **1** is in the solution containing a large excess of pyridine.

Obtained results for the three series with different alumazene-to-pyridine ratios are presented in Figure 5. For the sake of clarity, only data for heating runs are given. Due to the fact that prolonged heating at temperatures around 200 °C results in a slow decomposition in the system (seen by the loss of reproducibility of the subsequent heating/cooling runs and dark green discoloring of the sample), for the thermodynamic analysis only data for the first few heating runs were used in each series. The following processes were attributed to the exponential pressure increase:

$$\mathbf{1}(\mathrm{py})_3\ (\mathrm{s}) = \mathbf{1}(\mathrm{py})_2\ (\mathrm{s}) + \mathrm{py}\ (\mathrm{g}) \quad (1)$$

$$\mathbf{1}(\mathrm{py})_2\ (\mathrm{s}) = \mathbf{1}(\mathrm{py})\ (\mathrm{s}) + \mathrm{py}\ (\mathrm{g}) \quad (2)$$

For both equilibria, the equilibrium constant K^{eq} is equal to the partial pressure of the pyridine. Plot of the log K^{eq} versus 1000/T for the two processes is given in Figure 6S (see Supporting Information) and clearly indicates consistency between different experimental series, which allowed us to obtain the following thermodynamic characteristics. A dissociation of the first py molecule in process 1 within the temperature range 369−419 K is characterized by ΔH°_{T} 78 ± 3 kJ mol^{-1}, and ΔS°_{T} 180 ± 8 J mol^{-1} K^{-1}. At higher temperatures (435−468 K), values of 91 ± 3 kJ mol^{-1} and 191 ± 7 J mol^{-1} K^{-1} were obtained for ΔH°_{T} and ΔS°_{T}, respectively, for process 2. Summary of the experimentally obtained results for the solid **1**(py)$_n$ complexes is given in Table 3.

Computational Studies. Optimized structures of the model [HAlNH](py)$_n$ (n = 0−3) compounds are given in Figure 7S (see Supporting Information). Both *cis* and *trans* isomers were considered for [HAlNH](py)$_2$: the energy difference between isomers is small, and the *trans* isomer is favored by 5 kJ mol^{-1}. Summary of the results of theoretical studies is given in Table 4. The following trends were observed. For the gas-phase complexes upon increasing the number of donor ligands, the donor−acceptor distance Al−N(py) increases (2.095 < 2.110 < 2.123 Å for n = 1, 2, 3, respectively) in accord with decreasing donor−acceptor bond dissociation energy (87 > 75 > 63 kJ mol^{-1} for n = 1, 2, 3, respectively) or by about 12 kJ mol^{-1} for each step. These results are in qualitative agreement with the experimental trend for the stability of the solid **1**(py)$_n$ complexes (Table 3). In order to estimate the influence of the steric bulk, structures of the **1**(py)$_n$ complexes were fully optimized and verified to be true minima. Due to high computational demands, only *trans* isomers of **1**(py)$_2$ and **1**(py)$_3$ were considered. Structural changes are similar to that observed for the model complexes, but donor−acceptor bond lengths for complexes of **1** are substantially longer. Energetically, **1** is much weaker acceptor as compared to [HAlNH]$_3$. Especially noteworthy is a negative value of the dissociation enthalpy of the trisadduct **1**(py)$_3$ in the gas phase. Thus, existence of complex **1**(py)$_3$ in the gas phase is forbidden thermodynamically.

Conclusions

Alumazene **1** reveals its Lewis acidity at multiple Al centers and forms donor−acceptor bonds in the reactions with strong bases pyridine and dmap. The bisadducts **1**(py)$_2$, **1**(dmap)$_2$, and **1**(py)(dmap) feature only their *trans* isomers both in solution and solid state. The excess py is needed for isolation of trisadduct **1**(py)$_3$ as the third base dissociates easily. Dmap reveals its higher Lewis basicity in comparison to py in displaying shorter Al−N coordinative bonds and larger distortion from planarity of the Al coordination environment. A higher stability of the Al−dmap bonds over Al−py is demonstrated also in the solution NMR spectra. Thermodynamic characteristics were obtained by tensimetry for the dissociation of py from **1**(py)$_2$ and **1**(py)$_3$. Quantum chemical computations on the py complexes with model

compound $[HAlNH]_3$ and **1** in the gas phase have shown decreasing stability of the adducts with increasing number of py donors.

Acknowledgment. Financial support for this work by Grant MSM0021622410 is gratefully acknowledged.

Supporting Information Available: Complete X-ray data for compounds **2**−**5** in CIF format, listing of the $^{13}C\{^1H\}$ NMR spectra of **5**, and IR spectra of **2**, **4**, and **5**. Figures 6S and 7S. This material is available free of charge via the Internet at http://pubs.acs.org.

IC700488P